

# MTDH Activation by 8q22 Genomic Gain Promotes Chemoresistance and Metastasis of Poor-Prognosis Breast Cancer

Guohong Hu,<sup>1</sup> Robert A. Chong,<sup>1,6</sup> Qifeng Yang,<sup>2,6,7</sup> Yong Wei,<sup>1</sup> Mario A. Blanco,<sup>1</sup> Feng Li,<sup>1</sup> Michael Reiss,<sup>3,4</sup> Jessie L.-S. Au,<sup>5</sup> Bruce G. Haffty,<sup>2</sup> and Yibin Kang<sup>1,4,\*</sup>

<sup>1</sup>Department of Molecular Biology, Princeton University, Princeton, NJ 08544, USA

<sup>2</sup>Department of Radiation Oncology, Robert Wood Johnson Medical School, University of Medicine and Dentistry of New Jersey, New Brunswick, NJ 08901, USA

<sup>3</sup>Department of Internal Medicine

<sup>4</sup>Breast Cancer Program

The Cancer Institute of New Jersey, New Brunswick, NJ 08903, USA

<sup>5</sup>College of Pharmacy, The Ohio State University, Columbus, OH 43210, USA

<sup>6</sup>These authors contributed equally to this work

<sup>7</sup>Present address: Department of Breast Surgery, Qilu Hospital of Shandong University, Jinan, Shandong Province 250012, China

\*Correspondence: [ykang@princeton.edu](mailto:ykang@princeton.edu)

DOI 10.1016/j.ccr.2008.11.013

## SUMMARY

Targeted therapy for metastatic diseases relies on the identification of functionally important metastasis genes from a large number of random genetic alterations. Here we use a computational algorithm to map minimal recurrent genomic alterations associated with poor-prognosis breast cancer. 8q22 genomic gain was identified by this approach and validated in an extensive collection of breast tumor samples. Regional gain of 8q22 elevates expression of the metastasis gene metadherin (*MTDH*), which is overexpressed in more than 40% of breast cancers and is associated with poor clinical outcomes. Functional characterization of *MTDH* revealed its dual role in promoting metastatic seeding and enhancing chemoresistance. These findings establish *MTDH* as an important therapeutic target for simultaneously enhancing chemotherapy efficacy and reducing metastasis risk.

## INTRODUCTION

The progression of cancer from an abnormal outgrowth to a life-threatening metastatic tumor is accompanied by a myriad of genetic and epigenetic alterations accumulated along the way (Chin and Gray, 2008; Fidler, 2003; Gupta and Massagué, 2006; Hanahan and Weinberg, 2000; Steeg, 2006). The challenge of distinguishing crucial drivers of metastasis from thousands of bystander alterations remains a major bottleneck in metastasis research. The turn of the 21st century has witnessed the advent of two parallel but individually incomplete genomic

approaches to unravel the genetic mystery of cancer metastasis (Kang, 2005). Comparative expression profiling analyses of cancer cell line variants with different metastasis potentials, often obtained by in vivo selection in animal models, have led to the identification of several metastasis genes (Clark et al., 2000; Kang et al., 2003; Minn et al., 2005; Yang et al., 2004). However, much work remains to be done to validate the clinical relevance of metastasis genes identified in animal model studies. A second approach, gene expression profiling of human tumor specimens, has enabled the identification of several poor-prognosis signatures that are predictive of recurrence and metastasis risk in

## SIGNIFICANCE

Genomic profiling of breast cancer has established several clinically applicable poor-prognosis gene signatures. However, the lack of overlap between independent signatures prevents the identification of functionally important genes in the signatures. Here we report an integrative strategy to identify recurrent genomic alterations that are both clinically relevant and functionally important for breast cancer progression. Successful application of this approach led to the identification of metadherin (*MTDH*) at the recurrent 8q22 poor-prognosis genomic gain with important functions in both metastasis and chemoresistance. The dual functionality of *MTDH* further provides an explanation for the long-standing conceptual dilemma regarding the selection of metastasis genes in the primary tumor. Overall, our data illustrate the synergistic value of integrating bioinformatics with clinical and experimental metastasis research.

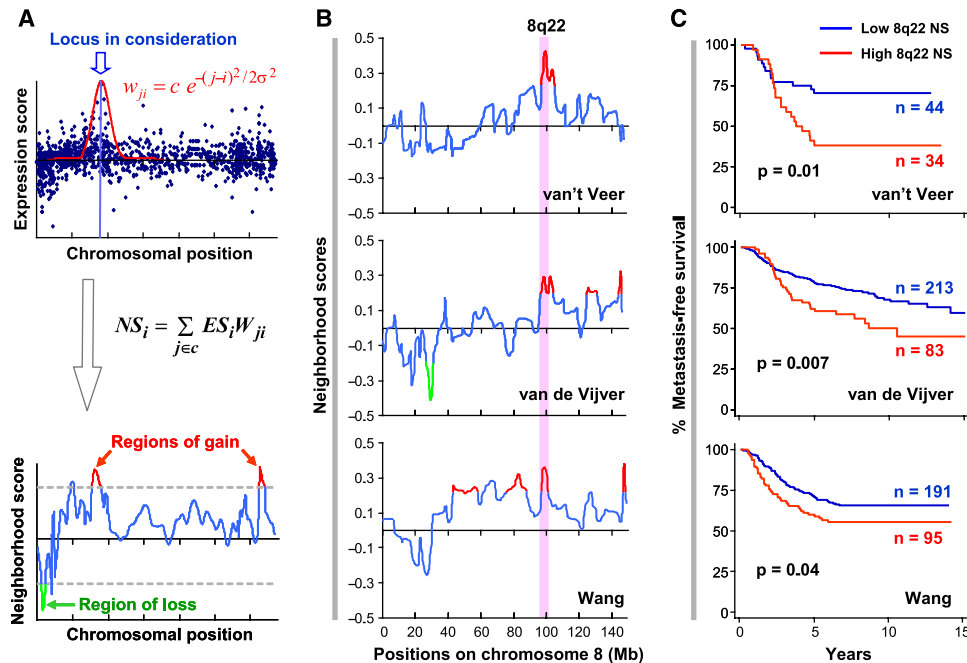


**Figure 1. ACE Analysis Identifies a Recurrent Genomic Gain at 8q22 in Poor-Prognosis Breast Cancer**

(A) In the ACE (analysis of CNAs by expression data) approach, the expression score (ES) of each gene is calculated by comparing samples of different phenotypes, and then a neighborhood score (NS), indicative of the DNA copy number status, is computed for each locus as the geometry-weighted ES sum of all of the genes on the chromosome. Regions of gain (red, bottom panel) and loss (green) were defined by applying NS cutoffs (dotted lines) obtained from permutations.  $i$  and  $j$ , gene index when genes are ordered on the chromosome by genomic positions;  $c$ , normalizing constant;  $w_{ji}$ , weight of gene  $j$  when locus  $i$  is in consideration (see text and Experimental Procedures for details).

(B) Poor-prognosis genomic gain at 8q22 was detected in all three data sets analyzed (van't Veer et al., 2002; van de Vijver et al., 2002; Wang et al., 2005). The traces are the NS scores on chromosome 8 produced by ACE. The shaded area highlights the consensus region of gain at 8q22. Red and green peaks represent statistically significant regions of gains and loss, respectively.

(C) Kaplan-Meier metastasis-free survival curves of patients with high or low 8q22 NS.

human cancers (Ramaswamy et al., 2003; van't Veer et al., 2002; van de Vijver et al., 2002; Wang et al., 2005). Although different poor-prognosis signatures have proven to be operationally interchangeable for class prediction purposes in the clinic (Fan et al., 2006), the lack of overlap between different poor-prognosis signatures has posed a major challenge for understanding the biological underpinnings of cancer progression and metastasis, thereby hindering the development of targeted therapeutics. Identifying functionally important and clinically relevant metastasis genes requires innovative strategies to synergize advances in both clinical and experimental metastasis studies.

Recurrent DNA copy number alterations (CNAs) have been observed in a wide range of human cancers, and such genetic events often indicate the presence of key mediators of malignancy in the affected genomic loci. For example, elevated expression of oncogenes, such as *c-Myc*, *CCND1*, *Her2*, and *EGFR1*, is often a result of amplification of their corresponding genomic segments (Chin and Gray, 2008). However, CNAs responsible for cancer metastasis are poorly characterized. Various techniques have been developed to detect genomic alterations, including fluorescence in situ hybridization (FISH), comparative genomic hybridization (CGH), and high-density single-nucleotide polymorphism (SNP) genotyping. Detection of CNAs by expression profiling analysis is theoretically possible since a strong correlation between genomic alterations and

aberrant expression of genes in affected loci has been observed (Pollack et al., 2002). Accurate detection of CNAs using expression analysis, however, is technically difficult because gene expression data reflect multiple layers of gene regulation beyond genomic alterations. Such analysis is particularly challenging with clinical tumor samples due to the inherent heterogeneity of clinical specimens and the rampant genomic instability of late-stage tumors. Here we used a computational algorithm to identify a recurrent genomic gain in poor-prognosis human breast cancers in 8q22, which harbors the metastasis gene *metadherin* (*MTDH*; also called *Lytic* and *AEG1* [Britt et al., 2004; Brown and Ruoslahti, 2004; Kang et al., 2005]). Functional characterization of *MTDH* revealed its dual functions in promoting metastasis and chemoresistance of breast cancers.

## RESULTS

### Recurrent Poor-Prognosis Genomic Alterations

To sensitively detect CNAs that affect regional gene expression, we developed a bioinformatic strategy called ACE (analysis of CNAs by expression data; Figure 1A). ACE first calculates the expression scores of all genes according to their expression differences between comparison groups and then orders them by genomic positions. To measure the regional expression pattern, a neighborhood score (NS) is calculated for each genomic locus

**Table 1. Recurrent Regions of Gain Associated with Poor-Prognosis Breast Cancer as Detected by ACE**

#	Location	Genomic Position (Mb)	Size (Mb)	Gene Number	Predicted in Data Sets
1	8q22	96.3–99.2	2.9	20	all
2	3q26.33–q27.1	180.2–184.4	4.2	27	Wang et al.; van't Veer et al.
3	8q24.3	144.4–145.7	1.3	82	Wang et al.; van de Vijver et al.
4	17q23.3–q25	54.8–58.2	3.4	42	Wang et al.; van de Vijver et al.
5	20q13.3	60.7–62.0	1.3	60	Wang et al.; van de Vijver et al.

using a geometry-weighted sum of expression scores of all the genes on the chromosome. The expression scores of the genes in proximity to the locus in consideration are assigned greater weights than those farther away because the locus linkage strength decays with distance. The significance of the NS is estimated by permutation, and regions with a stretch ( $\geq 20$ ) of aberrant NS are declared as potential CNA regions.

After validating the efficacy of the ACE method using a number of existing gene expression profiling data sets that have corresponding genomic alteration information (see Figure S1 and Supplemental Experimental Procedures available online), we applied it to the study of genomic alterations associated with poor prognosis of human breast cancer. Three separate studies have previously identified two poor-prognosis gene sets of 70 and 76 genes that can be used to robustly predict the clinical outcome of human breast cancers (van't Veer et al., 2002; van de Vijver et al., 2002; Wang et al., 2005). However, only a single gene (*CCNE2*) is present in both signatures. When the ACE method was applied to analyze these three data sets, five common genomic gains were observed in at least two data sets (Table 1), and 15 other genomic gains were observed in one of the three data sets (Table S1). The smallest regions of overlap (SROs) of common CNA events—namely, gains at 3q26–27, 8q22, 8q24.3, 17q23–25, and 20q13.3—are among a large number of genomic alterations previously observed in high frequencies in breast cancer, although their links to poor prognosis and tumor progression have not been established (Bergamaschi et al., 2006). We did not detect any genomic losses associated with more than one data set, which is consistent with previous observations that genomic gains are more prevalent than genomic losses in breast cancer, especially in patients with poor outcomes (Naylor et al., 2005). Out of the five prevalent genomic events, the 8q22 gain was consistently observed in all three data sets (Figure 1B). We calculated the NS of this region for each sample in the three data sets and used it to classify tumor samples into two groups with high and low NS. As shown in Figure 1C and Table S2, the probability of metastasis-free survival of patients with a high 8q22 NS was significantly lower than that of the control group in all three data sets. These analyses suggested that genomic gain of 8q22 is a strong predictor of poor prognosis in breast cancer.

During tumor progression, cancer cells usually acquire multiple genomic alterations. These genetic events may contribute to tumor aggressiveness independently or synergistically. To examine whether the other four regions interact with 8q22 gain in poor prognosis, we clustered the tumor samples in the three data sets according to the NS of the five regions (Figure S2). A significant fraction of samples with 8q22 gain also showed increased copy numbers at 8q24.3 ( $p < 0.01$ ,  $\chi^2$  test) in all three data sets, but no obvious link was found between 8q22 and

the other three regions. The concurrent copy number gains of the two 8q subregions is consistent with the previous observation of frequent genomic gain of the whole 8q arm in breast cancer tumors (Ried et al., 1995). However, survival analysis revealed no significant contribution of 8q24.3 to the prognostic power of 8q22, as patients with genomic gains at both regions displayed survival records similar to, or even better than, patients with 8q22 gain only (Figure S2), suggesting that 8q22 gain functions independently in poor prognosis.

#### Validation of 8q22 Genomic Gain in Breast Tumors

We used FISH and genomic DNA quantitative PCR (qPCR) to confirm 8q22 genomic gain in breast tumor samples. First, we analyzed a panel of microdissected tumor samples from fresh-frozen breast cancer specimens by qPCR using four pairs of primers that amplify DNA sequences on chromosome 8q21, q22, and q23 (Figures 2A and 2B). Out of 36 tumors, 10 (27.8%) were found to have aberrantly higher copy numbers ( $>3.6$ ) at 8q22 than the control human DNA sample (Table S3). As shown in Figure 2B, the ten genomic gain events spanned from 8q21 to 8q23 with a consensus region at 8q22, consistent with our computational prediction. DNA copy numbers detected by genomic qPCR analysis were consistent with FISH analysis of the same tumor specimens (Figure S3). To confirm the link between 8q22 genomic gain and elevated expression of genes located in this region, we used qRT-PCR to investigate the expression patterns of three genes at 8q22 (*PTDSS1*, *MTDH*, and *LAPTM4 $\beta$* ) in these tumors. A strong positive correlation was found between the expression of these genes and the 8q22 copy numbers (Figure 2B). Similar results were obtained when we analyzed a separate panel of 18 paraffin-embedded breast tumors (Table S3). Analysis of a panel of breast cancer cell lines also found a good correlation of 8q22 gain with a higher level of *MTDH* expression (Figure S3).

We further analyzed a breast cancer tissue microarray with detailed clinicopathological records by FISH using a bacterial artificial chromosome (BAC) probe located at the 8q22 region and found that 22 (26.8%) of the 82 hybridized primary tumor samples had an average 8q22 copy number larger than 3 (Figure 2C; Table S4). Notably, 8q22 gain was associated with a higher propensity of metastatic recurrence (Figure 2D). Together with the qPCR analysis described above, these data confirmed the ACE prediction that recurrent genomic gain at 8q22 leads to regional gene activation. More importantly, these results established 8q22 gain as a poor-prognosis marker event in breast cancer.

#### MTDH Promotes Breast Cancer Metastasis

There are 13 known genes and 7 hypothetical genes in the 8q22 poor-prognosis genomic gain region (Figure 2A). Overexpression of several genes in this region was independently linked to

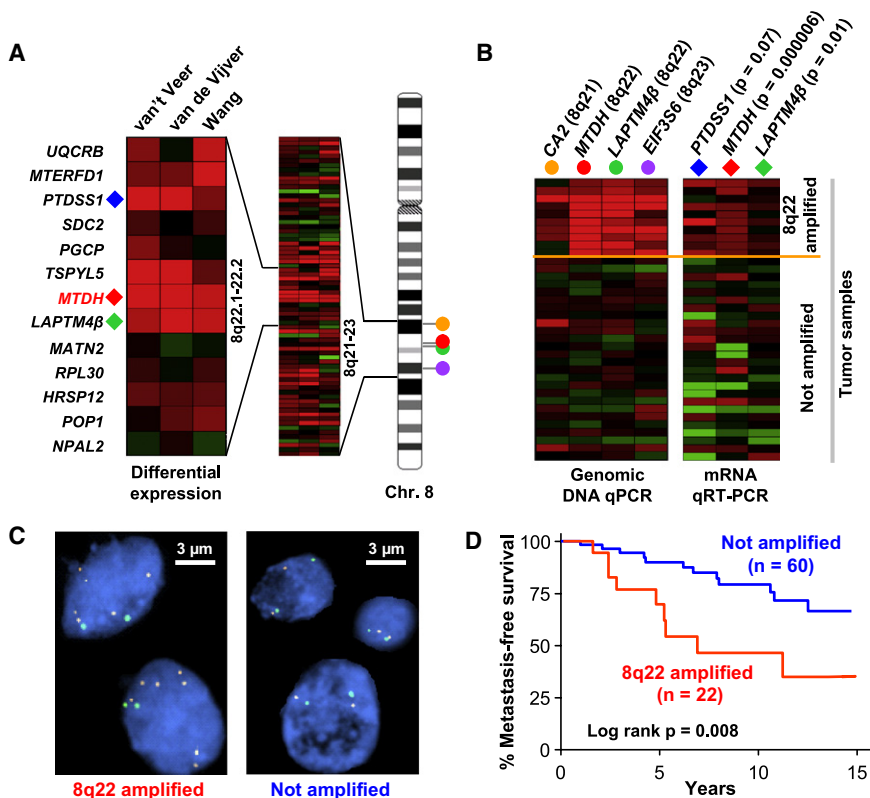


**Figure 2. Validation of 8q22 Genomic Gain in Human Breast Tumors**

(A) Expression of the genes at the 8q22 region in poor-prognosis versus good-prognosis samples of the three data sets. Red indicates overexpression; green indicates underexpression.

(B) To validate the 8q22 genomic gain, a panel of breast tumors were analyzed for 8q22 genomic alterations and gene expression using qPCR. DNA copy numbers of four genomic loci at 8q21-23 (circles) and expression levels of three genes at 8q22 (diamonds) are shown. Student's t test p values of expression comparison in samples with and without 8q22 gain are shown in parenthesis after each gene.

(C) Breast cancer tissue microarray fluorescence in situ hybridization (FISH) analysis with green SpectrumGreen and orange SpectrumOrange probes detecting the chromosome 8 centromere and the 8q22 region, respectively. A case of 8q22 gain (left) and a diploid case (right) are shown.

(D) Kaplan-Meier survival analysis in breast cancer patients with or without 8q22 gain.

poor prognosis in one or more data sets (Table S5). To determine the functional targets of 8q22 gain, we tested six known genes most likely to promote cancer progression based on statistical analysis and their known biological functions: *UQCRB*, *PTDSS1*, *TSPYL5*, *MTDH*, and *LAPTM4β*, which were significantly overexpressed in metastatic diseases in at least two of these data sets (Student's t test,  $p < 0.05$ ), and *SDC2*, which has been reported to mediate cell adhesion and proliferation in colon cancer (Park et al., 2002) (Figure S4). To test the role of these genes in metastasis, we stably overexpressed them in the SCP28 cell line, a subline of the human breast cancer cell line MDA-MB-231 that is mildly metastatic to lung and bone when injected into mice (Kang et al., 2003). The cell line was labeled with a retroviral construct expressing a GFP-luciferase fusion protein (Minn et al., 2005), and its in vivo metastasis capability was monitored by noninvasive bioluminescent imaging (BLI) after intravenous injection. Our data showed that *MTDH* overexpression significantly accelerated the development of lung metastasis and shortened the survival of mice that received tumor cell xenografts (Figures 3A–3D; Figure S4). Animal metastasis burden caused by *MTDH* overexpression was nearly 7-fold higher than the controls 6 weeks after cancer cell injection. In contrast, overexpression of the other five genes, either individually or in combination, failed to enhance the metastasis ability of SCP28 (Figure S4). Furthermore, overexpression of these genes together with *MTDH* did not further enhance lung metastasis beyond *MTDH* overexpression alone (Figure S4). Therefore, *MTDH* is likely to be the most significant functional mediator of this poor-prognosis genomic gain, although possible contributions from untested genes in the 8q22 region cannot be completely ruled out. *MTDH* is located

at the center of the minimal common region of the 8q22 genomic gain as indicated by the ACE computational analyses of three microarray data sets and has been shown to encode a cell surface protein responsible for promoting mouse mammary tumor cell adhesion to lung endothelial cells (Brown and Ruoslahti, 2004). However, the functional role of *MTDH* in human breast cancer and the mechanism of its deregulation have not been previously investigated.

To further validate the role of *MTDH* in metastasis, we used two different short-hairpin RNA (shRNA) constructs to knock down the expression of *MTDH* in the LM2 cell line, an MDA-MB-231 subline selected in vivo for its high lung metastasis propensity (Minn et al., 2005). The in vivo metastatic propensity of LM2 cells with *MTDH* knockdown was tested in nude mice after intravenous injection. *MTDH* knockdown significantly reduced the lung metastasis burden of LM2 by 3- to 5-fold and extended survival of the mice by 1–2 weeks (Figures 3A and 3E–3G; Figure S4). Histological analysis of primary tumors and lung metastases revealed poorly differentiated adenocarcinomas at both sites with very similar histological features (Figure S5). We further quantified the mRNA level of *MTDH* in cancer cells isolated from lung metastases (Figure S5). Cells isolated from lung lesions produced by *MTDH* knockdown cells continued to have a low level of *MTDH* expression, but modestly higher than the *MTDH* level in cells grown in culture, suggesting that the in vivo lung metastasis assay may select for “escapers” that have regained a higher level of *MTDH* expression.

We also examined the effect of altered *MTDH* expression on bone and brain metastasis by injecting the genetically modified breast cancer cell lines into the left cardiac ventricle of recipient nude mice. *MTDH* knockdown in LM2 resulted in a modest but significant improvement of postinjection survival, although bioluminescence quantification of the decrease of bone and brain

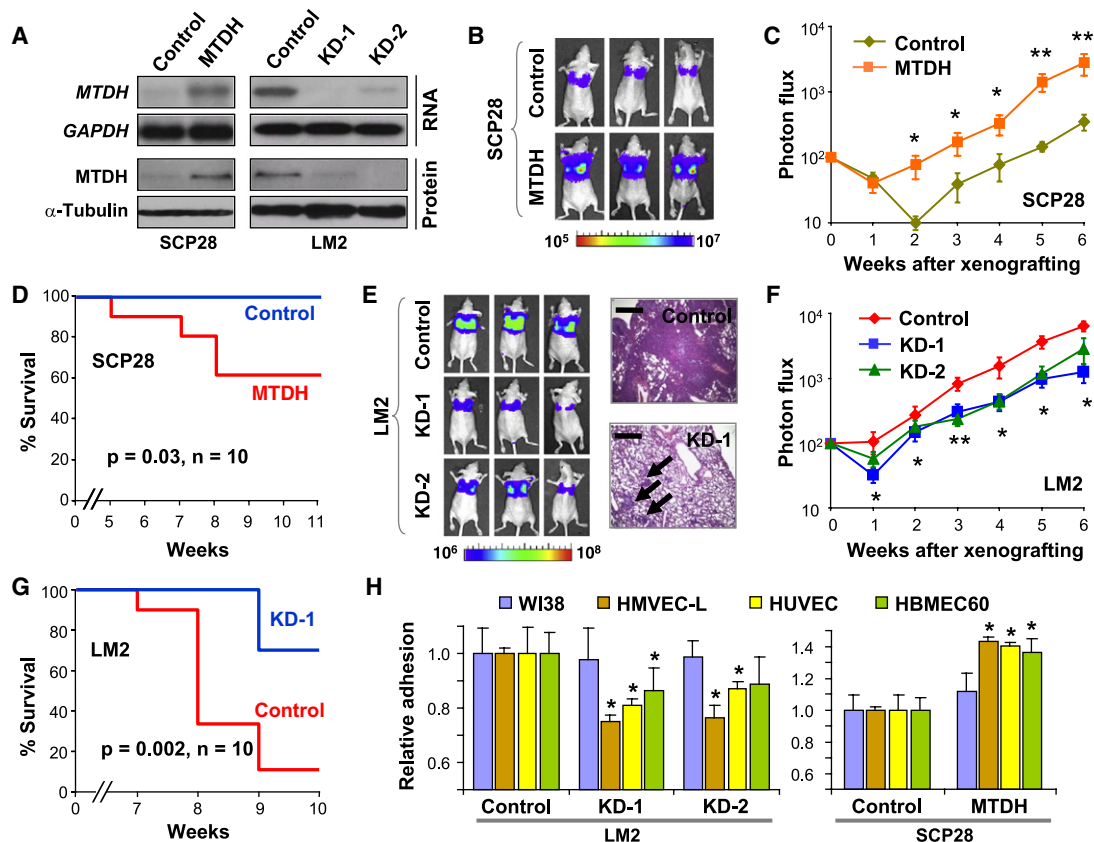


**Figure 3. MTDH Mediates Lung Metastasis of Human Breast Cancer**

(A) Metadherin (*MTDH*) is constitutively overexpressed in the mildly metastatic cell line SCP28 and stably knocked down in the highly lung-metastatic cell line LM2 with two independent short-hairpin constructs.

(B) In vivo metastasis assays of SCP28 cells with or without *MTDH* overexpression. Lung metastasis burden of xenografted animals was monitored weekly using bioluminescent imaging (BLI). Shown are BLI images of representative mice at the sixth week after injection. The color scale depicts the photon flux (photons per second) emitted from the metastasis cells.

(C) BLI quantification of lung metastasis of SCP28 cells.

(D) Kaplan-Meier survival curves of mice injected with SCP28 cells.

(E) Representative BLI images (left) and lung sections (right) of inoculated mice at the sixth week after injection of LM2 cells with or without *MTDH* knockdown. Arrows point to sporadic lesions by *MTDH* knockdown cells as compared to much more prevalent tumor lesions by control cells. Scale bars = 0.5 mm.

(F) BLI quantification of lung metastasis of LM2 cells. Data in (C) and (F) represent averages  $\pm$  SEM of 10 mice. \* $p < 0.05$ ; \*\* $p < 0.01$  by two-sided Wilcoxon rank test.

(G) Kaplan-Meier survival analysis of mice injected with LM2 cells.

(H) Genetically modified SCP28 or LM2 cells were seeded on top of a monolayer of endothelial cells from lung (HMVEC-L), umbilical vein (HUVEC), bone marrow (HBMEC60), and control fibroblast (WI38) cells, and the attached cells were quantified 3 hr later. Data represent averages  $\pm$  SEM.

metastasis burden did not reach statistical significance. Conversely, overexpression of *MTDH* in SCP28 cells led to a modest but significant increase of bone and brain metastasis (Figure S6). These results suggested that *MTDH* preferentially promotes metastasis to lung while having a modest effect on metastasis to other organs.

We further investigated the functional role of *MTDH* in the multistep process of metastasis. *MTDH* knockdown or overexpression did not affect the growth, migration, or invasiveness of various breast cancer cell lines, including MDA-MB-231 sublines (Figure S7), MCF7, and T47D (Figure S8 and data not shown). However, *MTDH* knockdown significantly reduced the adhesion of cancer cells to lung microvascular endothelial cells

(HMVEC-L), as well as to endothelial cells of the bone marrow (HBMEC60) and the umbilical vein (HUVEC), albeit to a lesser extent. A reciprocal change was observed when *MTDH* was overexpressed (Figure 3H). In contrast, the adhesion of cancer cells to the WI38 lung fibroblast cell line was not affected. *MTDH*-mediated enhancement of tumor cell adhesion to endothelial cells was also observed in other breast cancer cell lines, including MCF7 and T47D (Figure S8). *MTDH* did not promote intravasation or extravasation through endothelial layers based on both in vitro transendothelial assays and in vivo metastasis assays using an orthotopic xenograft method (data not shown). Instead, *MTDH* appeared to specifically enhance the seeding of tumor cells to the target organ endothelium.

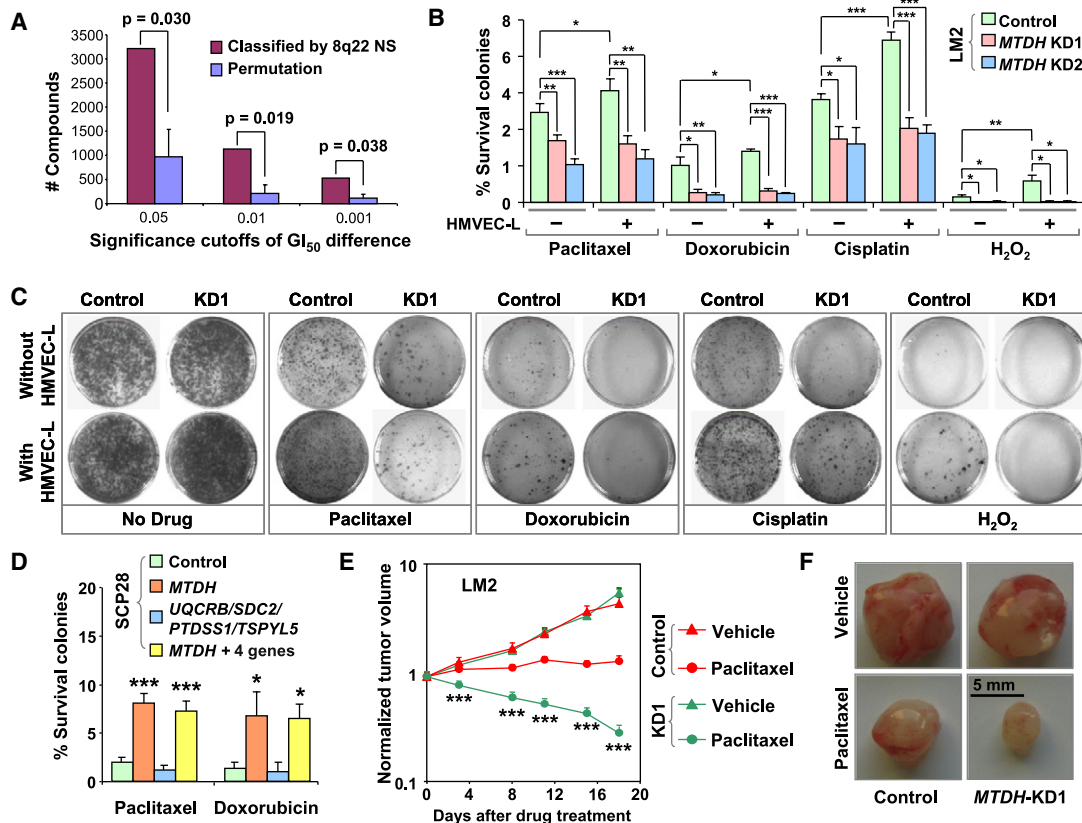


**Figure 4. MTDH Enhances Chemoresistance of Breast Cancer Cells**

(A) Genomic gain of 8q22 is associated with higher resistance to chemical compounds in the 58 human cancer cell lines. LogGI<sub>50</sub> (drug concentration for 50% growth inhibition) of each of the 24,642 compounds in cell lines with 8q22 gain was compared to those in cells without 8q22 gain. The numbers of compounds with significantly increased logGI<sub>50</sub> associated with 8q22 gain, counted by applying various significance thresholds of the logGI<sub>50</sub> differences ( $p < 0.05$ , 0.01, and 0.001), were compared to a null distribution obtained by permuting the 8q22 copy numbers of the cell lines. Median values from permutations are shown, with mean absolute deviation (MAD) as the error bar.

(B) Chemoresistance of LM2 cells was analyzed by clonogenic assays after treatment with various apoptosis-inducing agents with or without HMVEC-L coculture. Relative clonogenic abilities as percentages of the nontreatment control are shown.

(C) Representative images of clonogenic assays of LM2 cells.

(D) Clonogenic assays of SCP28 cells with overexpression of *MTDH* or other genes in the 8q22 region. Data with HMVEC-L coculture are shown.

(E) In vivo chemoresistance assay of LM2 cells. Xenograft tumor volumes in mice treated with paclitaxel or drug vehicle are shown ( $n = 6$  mice per group). Results in (B), (D), and (E) represent average values  $\pm$  SEM. \* $p < 0.05$ , \*\* $p < 0.01$ , \*\*\* $p < 0.001$  by two-sided Student's *t* test.

(F) Representative tumors isolated from mice 25 days after injection in the in vivo chemoresistance assay.

### MTDH Promotes Chemoresistance

Poor prognosis of breast cancer at the time of diagnosis or surgery indicates a higher probability of death as the result of recurrent tumors and development of metastases in vital organs. Emergence of metastasis reflects not only the ability of cancer cells to overcome hurdles during the multistep process of metastasis but also the capability to survive standard adjuvant therapy and other physiological stresses. Therefore, the driver gene of a poor-prognosis genetic alteration might function to promote chemoresistance in addition to enabling the metastasis process. A bioinformatic analysis of the available NCI60 pharmacogenomic data (Garraway et al., 2005) indicated a potential contribution of the genes at 8q22 to chemoresistance. The NCI60 data include the cytogenetic and expression profiles of 58 cancer cell lines as well as their sensitivity profiles to 24,000 small-molecule compounds. Analysis of these data revealed that genomic gain at 8q22 strongly correlated with a higher overall gene expression

of this region (Pearson's  $r = 0.578$ ; Figure S9); intriguingly, this higher NS was in turn associated with a significantly higher mean GI<sub>50</sub> (the drug concentration for 50% growth inhibition) for 1,123 compounds, as compared to  $211 \pm 178$  compounds expected by random permutation ( $p = 0.019$ ; Figure 4A). In contrast, copy number of the other 8q poor-prognosis region, 8q24.3, was not associated with any significant changes in GI<sub>50</sub> values (Figure S10). Similar analysis with the mRNA expression data of the genes at 8q22 revealed that *MTDH* is the only gene that has a significant correlation with higher chemoresistance (Table S6).

To investigate the chemoresistance function of *MTDH* and the other genes in 8q22, genetically modified LM2 breast cancer cell lines used for in vivo metastasis assays were treated with chemotherapeutic or other stress agents including paclitaxel, doxorubicin, cisplatin, and hydrogen peroxide with or without coculture with the HMVEC-L endothelial cell line. Long-term survival of

the cells was then quantified by clonogenic assays. Inhibition of *MTDH* expression sensitized the LM2 cell line to chemotherapeutic and stress agents, while overexpression of *MTDH* rendered SCP28 cells more resistant to these treatments (Figures 4B–4D). In contrast, overexpression of up to four other genes in the 8q22 locus did not significantly alter the chemosensitivity of cancer cells (Figure 4D). *MTDH*-dependent chemoresistance was further enhanced when cancer cells were cocultured with HMVEC-L endothelial cells (Figures 4B and 4C). *MTDH*-induced chemoresistance was not limited to the MDA-MB-231 cells, as *MTDH* knockdown in several additional breast cancer cell lines, including MCF7 and T47D, also significantly sensitized cells to chemotherapeutic challenges (Figure S8).

Next, we studied the chemoresistance function of *MTDH* in vivo using xenograft models. LM2 cells with or without *MTDH* knockdown were injected into nude mice subcutaneously. Twice-weekly treatment of tumors with paclitaxel or drug vehicle was initiated at 1 week after injection. Subcutaneous tumor volumes were monitored by direct caliper measurement. When the mice were treated with drug vehicle, the LM2 tumors grew rapidly, reaching five times the initial volume at 18 days after treatment (Figure 4E). Tumors from the *MTDH* knockdown cells grew at an equal rate, an observation consistent with the finding that *MTDH* does not affect primary tumor growth (Figure S7). Paclitaxel treatment significantly hampered tumor growth in mice injected with control LM2 cells. However, the tumors still grew to 140% in volume 18 days after treatment, indicating a considerable degree of chemoresistance in these cancer cells. *MTDH* knockdown significantly sensitized the cells to paclitaxel treatment, as tumor regression was observed immediately after the first treatment. The tumors eventually shrank to about 30% of pretreatment size 18 days after the initiation of treatment (Figures 4E and 4F). Similar results were obtained with another commonly used chemotherapeutic agent, doxorubicin (Figure S11).

### ALDH3A1 and MET Contribute to *MTDH*-Induced Chemoresistance

We performed drug uptake and retention assays for paclitaxel and doxorubicin in cancer cells with modified *MTDH* expression and found that *MTDH* did not change drug uptake or retention in these cells (Figure S12). Without a direct function in altering drug accumulation, *MTDH* may instead increase chemoresistance by promoting cellular survival against antineoplastic stresses. To further elucidate the molecular mechanism of *MTDH*-dependent chemoresistance, we compared gene expression profiles of two different *MTDH* knockdown LM2 cell lines against control cells. A similar comparison was also performed with LM2 cells cocultured with HMVEC-L cells (Figure 5A; Table S7). In the latter analysis, LM2 and HMVEC-L cells were labeled with GFP and seminaphthorhodafuor-1 (SNARF-1) dye, respectively, to allow fluorescence-activated cell sorting (FACS) of the two cell populations before RNA extraction (Figure 5B). Since *MTDH* induces significant chemoresistance with or without HMVEC-L coculture, we focused our attention on the significant genes (>2.5-fold change in expression; Student's *t* test  $p < 0.05$ ) that were consistently present in both conditions. Twenty-three genes (including *MTDH*) were found to be underexpressed in *MTDH* knockdown cells, while ten genes were overexpressed. Among the *MTDH*-

downregulated genes (i.e., genes upregulated following *MTDH* knockdown) were two cell death-inducing genes, *TRAIL* and *BINP3*. *TRAIL* encodes a TNF-family cytokine that induces apoptosis in tumor cells. Combining *TRAIL* with conventional anticancer drugs has been shown to improve therapeutic efficacy of chemotherapies (Ballestrero et al., 2004). *BNIP3* is a proapoptotic Bcl-2-family gene that has been shown to be involved in apoptotic, necrotic, and autophagic cell death (Mellor and Harris, 2007). Among the *MTDH*-upregulated genes were several genes previously implicated in chemoresistance of cancer cells, including *ALDH3A1*, *MET*, *HSP90AB1* (Bertram et al., 1996), *HSP90AB3P*, and *HMOX1* (Tanaka et al., 2003). The expression pattern of these genes in *MTDH* knockdown cells was confirmed by qPCR analysis using samples from both cell cultures and LM2 xenograft tumors (Figure 5C). The regulation of these genes by *MTDH* was additionally validated in three other breast cancer cell lines (MCF7, T47D, and BT474) using *MTDH* knockdown (Figure S8). Furthermore, a significant correlation of the expression of *MTDH* and its downstream genes was found in the NCI60 panel of human cancer cell lines as well as in primary breast tumor samples by computational analysis (Figure S13).

Among these candidate *MTDH* downstream genes, *ALDH3A1* (aldehyde dehydrogenase 3 family, member A1) and *MET* (hepatocyte growth factor receptor) are attractive targets because of their physiological functions and their expression patterns. Antineoplastic agents have been shown to produce oxidative stress in tumors during cancer chemotherapy. These effects are mediated in part by the generation of aldehydes that result from oxidative stress-induced lipid peroxidation. *ALDH3A1* encodes an antioxidant enzyme with several postulated protective roles that include detoxification of peroxidic aldehydes and scavenging of free radicals. Its expression has been implicated in clinical resistance to cyclophosphamide (Sreerama and Sladek, 2001), which is a mainstay of chemotherapeutic regimens used to treat breast cancers. Aldehyde dehydrogenase activity has also been shown to be a marker of cancer stem cells and may contribute to their increased chemoresistance (Croker et al., 2008; Ginestier et al., 2007). Interestingly, as revealed by microarray analysis (Figure 5A) and further confirmed by qRT-PCR (data not shown), *ALDH3A1* expression was 2- to 3-fold higher in the HMVEC-L coculture as compared to the non-coculture condition, while *MTDH* knockdown effectively repressed *ALDH3A1* expression in both conditions. Such an expression pattern matches the higher chemoresistance of cancer cells induced by HMVEC-L coculture and chemosensitization by *MTDH* knockdown in both conditions. To investigate the functional importance of *ALDH3A1* in *MTDH*-mediated chemoresistance, we engineered the LM2 cell line to express an inducible shRNA against *ALDH3A1* in order to produce conditional knockdown of *ALDH3A1*. LM2 cells were more sensitive to the chemotherapeutic agents paclitaxel, doxorubicin, and 4-hydroxycyclophosphamide (4-HC) when *ALDH3A1* knockdown was induced by addition of doxycycline, while release of *ALDH3A1* repression restored the chemoresistance of LM2 cells (Figure 5D).

We also tested the chemoresistance function of *MET*. In human patients, enhanced expression or activation of *MET* is observed in nearly all tumor types. In most cases, its expression is associated with both resistance to radio- and chemotherapy and poor prognosis (Birchmeier et al., 2003). In experimental

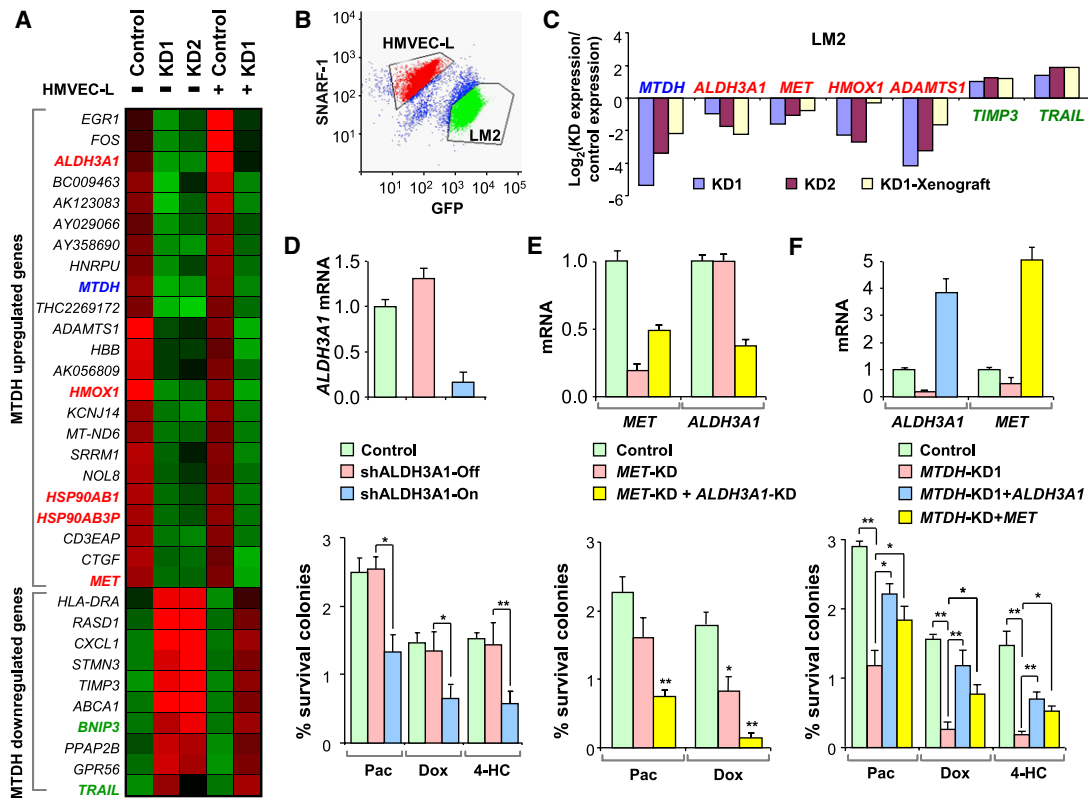


**Figure 5. ALDH3A1 and MET Contribute to MTDH-Mediated Chemoresistance**

(A) Expression pattern of genes regulated in *MTDH* knockdown cells with or without HMVEC-L coculture. Names of some genes previously implicated in promoting (red) or suppressing (green) cellular chemoresistance are highlighted. (B) In the coculture microarray experiment, HMVEC-L cells were prelabeled with seminaphthorhodafleur-1 (SNARF-1) dye and separated from GFP<sup>+</sup> LM2 cells by fluorescence-activated cell sorting (FACS) before microarray profiling. (C) qPCR analysis of the expression patterns of genes downregulated (red) or upregulated (green) in *MTDH* knockdown cells identified by microarray analysis. (D) *ALDH3A1* expression levels (top) and clonogenic assays (bottom) of cells engineered with *ALDH3A1*-inducible knockdown. (E) Gene expression (top) and clonogenic assays (bottom) of cells with *MET* knockdown or *MET* + *ALDH3A1* double knockdown. (F) Gene expression (top) and clonogenic assays (bottom) of *ALDH3A1* or *MET* overexpression rescue in LM2 cells with *MTDH* knockdown. In (D)–(F), data represent average ± SEM of three replicates. \**p* < 0.05, \*\**p* < 0.01 by two-sided Student's *t* test.

models, exogenous hepatocyte growth factor (HGF) or overexpression of *MET* induces resistance to ionizing radiation and many chemotherapeutics, including doxorubicin, cisplatin, etoposide, camptothecin, paclitaxel, TNF, and gefitinib, in diverse human cancer cells from different tumor types, as well as in endothelial cells (Engelman et al., 2007; Wei and Au, 2005). *MET* knockdown in LM2 cells led to a significant reduction of chemoresistance to doxorubicin, an effect similar to but weaker than that of *MTDH* knockdown (Figure 5E). When *MET* and *ALDH3A1* were simultaneously knocked down in LM2 cells, the chemosensitizing effects reached a level comparable to that of *MTDH* knockdown (Figure 5E). We further tested the ability of *ALDH3A1* and *MET* to rescue the chemoresistance phenotype in *MTDH* knockdown cells. Constitutive overexpression of *ALDH3A1* or *MET* in the *MTDH* knockdown cells was able to partially rescue the chemoresistance of LM2 cells to paclitaxel, doxorubicin, and 4-HC (Figure 5F). Together, these results suggest that *ALDH3A1* and *MET* are among the *MTDH* downstream genes that collectively contribute to its role in broad-spectrum chemoresistance.

### MTDH Correlates with Poor Prognosis in Clinical Samples

To evaluate the clinical importance of *MTDH* in breast cancer, we stained the tissue microarray used in the previous FISH analysis using an antibody against *MTDH*. Among the 170 samples on the tissue microarray, 47% expressed *MTDH* at a moderate to high level (Figure 6A). Overexpression of *MTDH* was not linked to any specific breast tumor subtype in terms of HER2 status, triple marker status (ER/PR/HER2), or the basal epithelial cell marker CK5/6 status (Figure S14) but was significantly associated with a higher risk of metastasis (log rank, *p* = 0.0058) and shorter survival time (*p* = 0.0008). Univariate survival analysis using the Cox proportional hazards model also suggested that high *MTDH* expression is strongly associated with a higher hazard ratio (HR) and worse clinical outcomes (HR = 3.7, *p* = 0.01 for metastasis; HR = 8.3, *p* = 0.005 for cancer-related death). Of note, immunohistochemical analysis of CCNE2 protein expression (encoded by the only gene present in both poor-prognosis signatures identified by van't Veer et al. [2002] and Wang et al. [2005]) in the same breast tumor tissue array did not reveal any significant



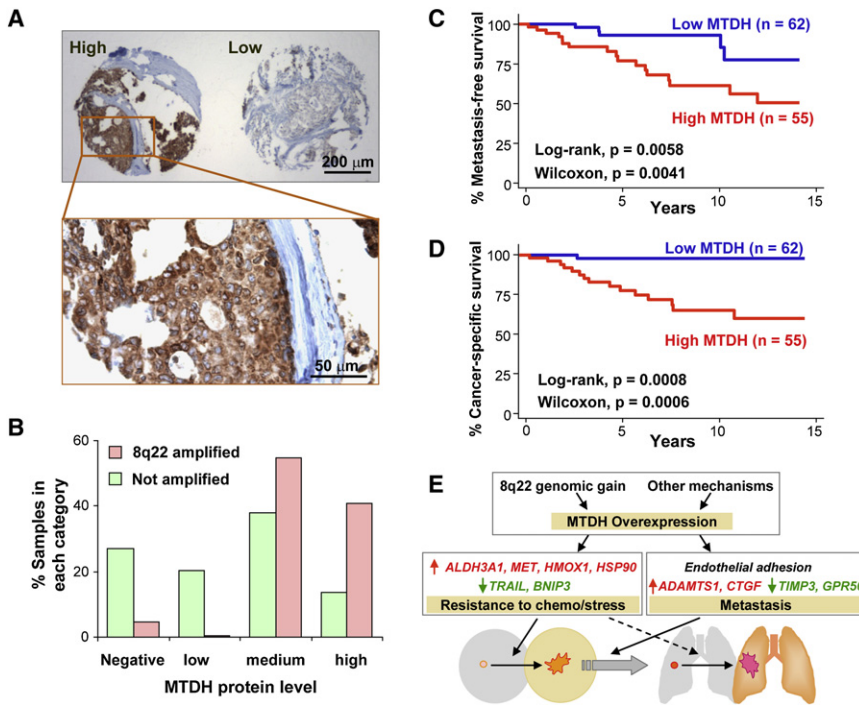


**Figure 6. MTDH Is Associated with Poor Prognosis of Human Breast Tumors**

(A) Typical MTDH immunostaining images of a human breast cancer tissue microarray. (B) MTDH protein levels are positively correlated with FISH 8q22 DNA copy numbers. (C) High MTDH protein level is associated with early metastasis in cancer patients. (D) High MTDH expression is also associated with worse cancer-specific survival. (E) A schematic model for the dual role of MTDH in breast cancer progression. In poor-prognosis tumors, 8q22 genomic gain leads to overexpression of MTDH, which in turn activates two parallel programs to promote chemoresistance and metastasis. Elevated expression of the chemoresistance genes *ALDH3A1*, *MET*, *HMOX1*, and *HSP90*, as well as repression of the apoptosis-inducing genes *TRAIL* and *BNIP3*, promotes the survival and outgrowth of cancer cells in the primary site as well as secondary organs in the face of physiological stress and chemotherapeutic challenges. MTDH additionally promotes metastasis by mediating tumor cell adhesion through interactions with unknown receptors and by activating prometastasis genes and suppressing metastasis-suppressing genes. Some of the molecular mediators of MTDH function may play a role in both functional categories. For example, *MET* can promote both metastasis and chemoresistance, and endothelial adhesion can further enhance MTDH-mediated chemoresistance.

correlation with metastasis (Figure S15). Interestingly, *CCNE2* is located in very close proximity to the recurrent 8q22 genomic gain (Figure S15; Table S5). It is possible that the recurrent presence of *CCNE2* in multiple poor-prognosis signatures is due to its close physical linkage to 8q22.

We further analyzed the correlation of MTDH protein levels with 8q22 DNA copy numbers using the samples with both successful immunostaining and FISH results. While the data showed that all but one of the tumors with 8q22 gain expressed abundant (medium or high) levels of MTDH protein (Figure 6B;  $\chi^2$  test  $p < 0.001$ ), a substantial fraction (12%) of samples with normal DNA copy numbers also had high levels of MTDH protein. Therefore, alternative mechanisms distinct from 8q22 gain may also result in *MTDH* activation in breast tumors. Nevertheless, survival analysis of the tumor samples in our tissue microarray and in the three previously published data sets consistently showed that *MTDH* activated by genomic gain or other means leads to similar clinical outcomes (Figure S16).

To further analyze the prognostic significance of MTDH, we performed Cox hazard ratio analysis of MTDH expression with the tissue samples stratified by other common clinicopathological parameters including ER, PR, HER2, and p53 status as well as the sizes of primary tumors at the time of cancer diagnosis (Table 2). MTDH expression level retained its prognostic significance in these analyses, suggesting that it is a prognostic factor independent of other clinicopathological factors. Indeed, a multivariate Cox analysis combining all of the above parameters with MTDH expression showed that the hazard of metastasis was still significantly higher with MTDH expression ( $p = 0.023$ ) even when all of the other factors were considered.

## DISCUSSION

In this study, we used the ACE algorithm to unveil functionally significant cytogenetic events directly linked to altered gene expression in poor-prognosis tumors. High-throughput genomic profiling methods such as array CGH (aCGH) and SNP arrays have facilitated the recent discovery of several cancer genes (Garraway et al., 2005; Kim et al., 2006). As an addition to the repertoire of integrative genomic analysis tools, ACE is particularly useful when cytogenetic data are not available, or it can be used as a complementary strategy to fine map results obtained from cytogenetic analyses and help narrow the list of genes for functional analysis. A further advantage of ACE is that it can detect regional epigenetic alterations that cannot be discerned by the aCGH or SNP array approaches (Figure S1). Additionally, ACE provides a direct link between cytogenetic events and gene activity changes, thereby facilitating the search for functionally important candidate genes. Given the large amount of archived gene expression data available in the public domain and the difficulty in obtaining matched cancer samples, ACE will be a useful data mining tool to complement the direct copy number detection methods to help shed light on the functional mechanism of cancer progression.

Our ACE analysis of breast cancer, together with clinical and functional studies of MTDH, strongly suggests that *MTDH* is a metastasis gene with great prognostic potential and therapeutic value. Brown et al. previously used phage display to identify MTDH as a homing receptor that mediates the adhesion of the 4T1 murine mammary tumor cell line to lung endothelial cells and promotes lung metastasis (Brown and Ruoslahti, 2004). In

**Table 2. Cox Hazard Ratios for Metastasis in Breast Cancer Based on MTDH Expression Levels in Tissue Array Analysis**

Pathological Parameter	MTDH Hazard Ratio in Stratified Analysis <sup>a</sup>		Multivariate Analysis <sup>b</sup>	
	Hazard Ratio (95% CI)	p Value	Hazard Ratio (95% CI)	p Value
MTDH	3.70 (1.36–10.0)	0.010	4.28 (1.32–13.9)	0.015
ER	3.91 (1.30–11.8)	0.015	3.13 (0.59–16.5)	0.180
PR	3.84 (1.27–11.6)	0.016	0.682 (0.17–3.76)	0.800
HER2	3.20 (1.20–9.99)	0.026	4.79 (1.75–19.6)	0.030
p53	4.09 (1.34–12.5)	0.012	0.60 (0.19–1.94)	0.400
ER+PR+HER2	2.47 (1.25–9.56)	0.017	3.15 (0.51–19.3)	0.200
Tumor size	4.21 (1.28–12.5)	0.007	2.38 (0.87–6.52)	0.090

<sup>a</sup> Univariate analysis of MTDH expression alone (first data row) or stratified by the indicated second parameter (all other data rows).

<sup>b</sup> Multivariate analysis of all parameters, including MTDH, ER, PR, HER2, p53, and tumor size.

that study, only the mouse 4T1 cell line and the biologically irrelevant HEK293T cell line were used to analyze the lung-targeting function of MTDH. The involvement of MTDH in human cancer, however, has not been previously reported. In this study, we used an extensive collection of human breast tumor samples to demonstrate that elevated MTDH protein level is an important prognostic factor independent of other clinicopathological factors. Our results indicated that a substantial proportion of human breast tumors exhibit *MTDH* genomic copy gains with a subsequent increase in *MTDH* expression, which is clearly associated with poor survival and higher risk of progression. We further firmly validated the functional importance of MTDH in systemic metastasis using a well-established model for human breast cancer metastasis. The importance of MTDH in cancer metastasis might not be limited to promoting lung-specific spread of breast tumor cells. Although MTDH was previously reported to enhance murine mammary tumor cell adhesion to lung endothelial cells (Brown and Ruoslahti, 2004), we showed that MTDH also enhances the adhesion of human breast cancer cells to other endothelial cell types, consistent with its function to increase systemic metastasis in vivo of a mildly metastatic cell line. However, *MTDH* overexpression alone in nonmetastatic breast cancer cell lines, including BT20, ZR-75-1, and ZR-75-30, was not sufficient to allow these cells to gain metastatic ability in animal assays (data not shown). This is consistent with recent studies showing that simultaneous overexpression of multiple metastasis genes is often required to achieve high metastatic capabilities (Gupta et al., 2007; Kang et al., 2003; Minn et al., 2005). Nevertheless, our in vitro, in vivo, and clinical studies firmly established MTDH as an appealing target for therapeutic intervention of metastatic diseases.

Current standard treatment for breast cancer uses the combination of surgery to remove localized disease and chemotherapy to eliminate systemic spreading. However, relapsed breast cancers almost invariably acquire resistance to chemotherapy and are often inoperable. Thus, over 90% of breast cancer-related deaths are due not to cancer at the primary site but rather to the spread of chemoresistant cancer cells from the breast to secondary vital organs such as lung, bone, liver, and brain. Metastasis and chemoresistance remain two major challenges to curative therapy. Our study uncovered a role for MTDH in chemoresistance of cancer cells. Thus, *MTDH* may be among an important class of genes that play dual roles in metastasis and chemoresistance (Figure 6E). This may explain why some of the metastasis

genes are selected for in the primary tumor—presumably as a consequence of their ability to endow cancer cells with enhanced tolerance to therapeutic and physiological stresses that human tumors may endure—but do not confer an apparent growth advantage in animal tumorigenesis assays (Bernards and Weinberg, 2002). In addition to promoting chemoresistance of primary tumors, MTDH may also increase the risk of metastatic recurrence by enhancing the survival of metastatic lesions against chemotherapy (Figure 6E), although this was not proven directly in our current study due to difficulty in segregating the two functions (metastasis and chemoresistance) of MTDH in the in vivo metastasis assays. Ongoing studies in our laboratory have also validated the dual functions of MTDH in metastasis and chemoresistance in prostate cancer (G.H., Y.W., R.A.C., Q.Y., J. Siddiqui, K.J. Pienta, and Y.K., unpublished data), suggesting a potential broader functional involvement of MTDH in the progression of a variety of cancers.

Microarray profiling of *MTDH* knockdown cells revealed several genes, including *ALDH3A1* and *MET*, that collectively contribute to the multidrug chemoresistance function of MTDH. Several other genes identified by the microarray experiment may also contribute to the prometastasis function of MTDH. For example, genes that are downregulated by *MTDH* inhibition include several previously reported metastasis-promoting genes such as *MET*, *ADAMTS1*, and *CTGF* (Kang et al., 2003; Lorenzato et al., 2002). Conversely, several genes that have been reported to suppress metastasis, including *GPR56*, *TIMP3*, and *TRAIL* (Lin et al., 2002; Manka et al., 2005; Xu et al., 2006), were overexpressed in the *MTDH* knockdown line (Figure 5A; Table S7). The mechanism of regulation of these downstream genes by MTDH and the identification of the functional partners of MTDH will be important matters to be addressed by future studies.

In conclusion, we have used a combination of computational biology, in vivo and in vitro functional metastasis assays, and extensive clinical correlation analyses to identify the 8q22 poor-prognosis genomic gain that harbors the dual-function metastasis gene *MTDH*. Overexpression of *MTDH* occurs in up to 40% of breast cancer patients and promotes metastatic seeding as well as chemoresistance of breast tumors. There are several potential applications of this study in the clinical management of human breast cancer. Genomic gain and overexpression of *MTDH* can become a powerful prognosis marker independent from other well-established markers for breast cancer. Molecular targeting of *MTDH* may not only prevent the seeding of breast

cancer cells to the lung and other vital organs but also sensitize cancer cells to chemotherapy, thereby stopping the deadly spread of breast cancer.

## EXPERIMENTAL PROCEDURES

### Development of ACE Algorithm

ACE (analysis of CNAs by expression data) detects genetic alterations in three steps: (1) calculating neighborhood scores (NS) for each chromosomal locus as an indicator of copy number alteration (CNA) likelihood at that locus; (2) estimating the significance of the NS; and (3) defining the regions of gain and loss.

The expression score (ES) for each gene is first calculated according to the correlation of its expression with the phenotypes in comparison. In this manuscript, paired t statistics (for ovarian cancer cell lines) or independent t statistics (for other data sets) were used to score gene expression. In general, other metrics can also be used. Consider the genes 1, 2, ..., N on a chromosome ordered by their physical positions. We define the NS at locus *i* as the weighted sum of the ES of this chromosome:

$$NS_i = \sum_{j=1}^N w_{ji} ES_j,$$

where  $w_{ji}$  is the weight of gene *j*. Because the linkage strength between two loci becomes weaker as the distance increases, the weight  $w_{ji}$  decreases when locus *j* is farther away from the locus *i*. The contribution from each gene is weighted by a Gaussian function:

$$W_{ji} = ce^{-|j-i|^2/2\sigma^2},$$

where *c* is a constant to normalize all NS into a range of [−1, 1]. The variation parameter  $2\sigma^2$  controls the weight decay rate and was arbitrarily set to 100 in the analyses presented here. An analysis using varying  $2\sigma^2$  values from 20 to 200 showed similar results, with slight shifts at the boundaries of detected regions. For each locus, only the genes in its physical proximity will have measurable influence on its NS because of weight decay. Positive and negative NS suggest genomic gain and loss, respectively. To evaluate the significance of the NS, the gene positions (or sample class labels, if the sample size is large enough) are permuted 1000 times, and each time the NS are recomputed. The p values of observed NS are then computed using the distribution of permuted NS and adjusted to false discovery rate (FDR) q values by the Benjamini-Hochberg procedure. In all of the CNA analyses presented in this manuscript, we defined a region of genomic gain as one with at least 20 continuous positive NS of FDR  $q < 0.01$ , or a region of genomic loss as one in which such NS are all negative. In the epigenetic analysis, we used a cutoff of five continuous NS, as epigenetic regulation usually has a smaller functioning range.

ACE has been implemented as a software tool to analyze expression data obtained from various array platforms and is available in the [Supplemental Data](#) online.

### Tumorigenesis and Metastasis Assays in Nude Mice

All animal work was performed in accordance with the guidelines of the Institutional Animal Care and Use Committee of Princeton University under approved protocols.  $2 \times 10^5$  cells were washed in PBS and injected intravenously into female athymic Ncr-nu/nu mice to study lung metastasis activity as described previously (Minn et al., 2005). For bone metastasis analysis,  $1 \times 10^5$  cells were injected into the left ventricle of the heart as described previously (Kang et al., 2003). Noninvasive bioluminescence imaging was performed to quantify the metastasis burden in the target organs using an IVIS 200 Imaging System (Caliper Life Sciences) as described previously (Minn et al., 2005).

To study primary tumorigenesis, cancer cells harvested from culture were resuspended in PBS at a concentration of  $1 \times 10^7$  cells/ml. An incision was made in the abdomen, and the skin was recessed to locate the #4 mammary fat pad, into which  $10^5$  cells ( $10 \mu\text{l}$ ) were injected under a dissection microscope. Primary tumor volume was monitored weekly as described previously (Minn et al., 2005).

### Human Tumor Samples

Tumor specimens were obtained from the Cancer Institute of New Jersey with informed consent from all subjects in accordance with the institutional review

boards of Princeton University and the University of Medicine and Dentistry of New Jersey. Details on the characterization of each tumor specimen can be found in [Supplemental Experimental Procedures](#).

### Statistical Analysis

The Kaplan-Meier method was used to estimate survival curves for human patients and animals. Log-rank test and Wilcoxon test were used to compare the differences between curves. Two-sided Wilcoxon rank test was performed to analyze the bioluminescence imaging results in the in vivo studies. A two-sided independent Student's t test without equal variance assumption was performed to analyze the results of luciferase assays and clonogenic assays.

### ACCESSION NUMBERS

Microarray data reported herein have been deposited at the NCBI Gene Expression Omnibus (<http://www.ncbi.nlm.nih.gov/geo/>) with the accession number GSE9187.

### SUPPLEMENTAL DATA

The Supplemental Data include Supplemental Experimental Procedures, Supplemental References, nine tables, sixteen figures, and the ACE software package and can be found with this article online at [http://www.cancerell.org/supplemental/S1535-6108\(08\)00379-6](http://www.cancerell.org/supplemental/S1535-6108(08)00379-6).

### ACKNOWLEDGMENTS

We thank J. Massagué, D. Botstein, S. Tavazoie, Y. Shi, and O. Matveeva for insightful discussions and technical suggestions; L.M. Staudt for the pRSMX vector; C.J. Kirkpatrick for the STA cell line; L. Cong, J. Friedman, and L. Goodell at the Tissue Analytic Services Shared Resource of the Cancer Institute of New Jersey for assistance with immunohistochemistry analysis of tissue arrays; and Y. Xiao, K. Jones, and C. Lee at the Dana-Farber Cancer Institute Cytogenetics Core for FISH analysis. Y.K. was funded by a Department of Defense Era of Hope Scholar Award and grants from the NIH (R01CA134519), the American Cancer Society, the Susan G. Komen Foundation, and the New Jersey Commission on Cancer Research. G.H. is supported by a postdoctoral fellowship from the New Jersey Commission on Cancer Research.

Received: June 17, 2008

Revised: September 8, 2008

Accepted: November 19, 2008

Published: January 5, 2009

### REFERENCES

- Ballestrero, A., Nencioni, A., Boy, D., Rocco, I., Garuti, A., Mela, G.S., Van Parijs, L., Brossart, P., Wesselborg, S., and Patrone, F. (2004). Tumor necrosis factor-related apoptosis-inducing ligand cooperates with anticancer drugs to overcome chemoresistance in antiapoptotic Bcl-2 family members expressing jurkat cells. *Clin. Cancer Res.* 10, 1463–1470.
- Bergamaschi, A., Kim, Y.H., Wang, P., Sorlie, T., Hernandez-Boussard, T., Lonning, P.E., Tibshirani, R., Borresen-Dale, A.L., and Pollack, J.R. (2006). Distinct patterns of DNA copy number alteration are associated with different clinicopathological features and gene-expression subtypes of breast cancer. *Genes Chromosomes Cancer* 45, 1033–1040.
- Bernards, R., and Weinberg, R.A. (2002). A progression puzzle. *Nature* 418, 823.
- Bertram, J., Palfner, K., Hiddemann, W., and Kneba, M. (1996). Increase of P-glycoprotein-mediated drug resistance by hsp 90 beta. *Anticancer Drugs* 7, 838–845.
- Birchmeier, C., Birchmeier, W., Gherardi, E., and Vande Woude, G.F. (2003). Met, metastasis, motility and more. *Nat. Rev. Mol. Cell Biol.* 4, 915–925.
- Britt, D.E., Yang, D.F., Yang, D.Q., Flanagan, D., Callanan, H., Lim, Y.P., Lin, S.H., and Hixson, D.C. (2004). Identification of a novel protein, LYRIC, localized to tight junctions of polarized epithelial cells. *Exp. Cell Res.* 300, 134–148.

- Brown, D.M., and Ruoslahti, E. (2004). Metadherin, a cell surface protein in breast tumors that mediates lung metastasis. *Cancer Cell* 5, 365–374.
- Chin, L., and Gray, J.W. (2008). Translating insights from the cancer genome into clinical practice. *Nature* 452, 553–563.
- Clark, E.A., Golub, T.R., Lander, E.S., and Hynes, R.O. (2000). Genomic analysis of metastasis reveals an essential role for RhoC. *Nature* 406, 532–535.
- Crocker, A.K., Goodale, D., Chu, J., Postenka, C., Hedley, B.D., Hess, D.A., and Allan, A.L. (2008). High aldehyde dehydrogenase and expression of cancer stem cell markers selects for breast cancer cells with enhanced malignant and metastatic ability. *J. Cell. Mol. Med.* Published online August 4, 2008. 10.1111/j.1582-4934.2008.00455.x.
- Engelman, J.A., Zejnullahu, K., Mitsudomi, T., Song, Y., Hyland, C., Park, J.O., Lindeman, N., Gale, C.M., Zhao, X., Christensen, J., et al. (2007). MET amplification leads to gefitinib resistance in lung cancer by activating ERBB3 signaling. *Science* 316, 1039–1043.
- Fan, C., Oh, D.S., Wessels, L., Weigelt, B., Nuyten, D.S., Nobel, A.B., van't Veer, L.J., and Perou, C.M. (2006). Concordance among gene-expression-based predictors for breast cancer. *N. Engl. J. Med.* 355, 560–569.
- Fidler, I.J. (2003). The pathogenesis of cancer metastasis: the 'seed and soil' hypothesis revisited. *Nat. Rev. Cancer* 3, 453–458.
- Garraway, L.A., Widlund, H.R., Rubin, M.A., Getz, G., Berger, A.J., Ramaswamy, S., Beroukhi, R., Milner, D.A., Granter, S.R., Du, J., et al. (2005). Integrative genomic analyses identify MITF as a lineage survival oncogene amplified in malignant melanoma. *Nature* 436, 117–122.
- Ginestier, C., Hur, M.H., Charafe-Jauffret, E., Monville, F., Dutcher, J., Brown, M., Jacquemier, J., Viens, P., Kleer, C.G., Liu, S., et al. (2007). ALDH1 is a marker of normal and malignant human mammary stem cells and a predictor of poor clinical outcome. *Cell Stem Cell* 1, 555–567.
- Gupta, G.P., and Massagué, J. (2006). Cancer metastasis: building a framework. *Cell* 127, 679–695.
- Gupta, G.P., Nguyen, D.X., Chiang, A.C., Bos, P.D., Kim, J.Y., Nadal, C., Gomis, R.R., Manova-Todorova, K., and Massagué, J. (2007). Mediators of vascular remodelling co-opted for sequential steps in lung metastasis. *Nature* 446, 765–770.
- Hanahan, D., and Weinberg, R.A. (2000). The hallmarks of cancer. *Cell* 100, 57–70.
- Kang, D.C., Su, Z.Z., Sarkar, D., Emdad, L., Volsky, D.J., and Fisher, P.B. (2005). Cloning and characterization of HIV-1-inducible astrocyte elevated gene-1, AEG-1. *Gene* 353, 8–15.
- Kang, Y. (2005). Functional genomic analysis of cancer metastasis: biologic insights and clinical implications. *Expert Rev. Mol. Diagn.* 5, 385–395.
- Kang, Y., Siegel, P.M., Shu, W., Drobnjak, M., Kakonen, S.M., Cordon-Cardo, C., Guise, T.A., and Massagué, J. (2003). A multigenic program mediating breast cancer metastasis to bone. *Cancer Cell* 3, 537–549.
- Kim, M., Gans, J.D., Nogueira, C., Wang, A., Paik, J.H., Feng, B., Brennan, C., Hahn, W.C., Cordon-Cardo, C., Wagner, S.N., et al. (2006). Comparative oncogenomics identifies NEDD9 as a melanoma metastasis gene. *Cell* 125, 1269–1281.
- Lin, T., Huang, X., Gu, J., Zhang, L., Roth, J.A., Xiong, M., Curley, S.A., Yu, Y., Hunt, K.K., and Fang, B. (2002). Long-term tumor-free survival from treatment with the GFP-TRAIL fusion gene expressed from the hTERT promoter in breast cancer cells. *Oncogene* 21, 8020–8028.
- Lorenzato, A., Olivero, M., Patane, S., Rosso, E., Oliaro, A., Comoglio, P.M., and Di Renzo, M.F. (2002). Novel somatic mutations of the MET oncogene in human carcinoma metastases activating cell motility and invasion. *Cancer Res.* 62, 7025–7030.
- Manka, D., Spicer, Z., and Millhorn, D.E. (2005). Bcl-2/adenovirus E1B 19 kDa interacting protein-3 knockdown enables growth of breast cancer metastases in the lung, liver, and bone. *Cancer Res.* 65, 11689–11693.
- Mellor, H.R., and Harris, A.L. (2007). The role of the hypoxia-inducible BH3-only proteins BNIP3 and BNIP3L in cancer. *Cancer Metastasis Rev.* 26, 553–566.
- Minn, A.J., Gupta, G.P., Siegel, P.M., Bos, P.D., Shu, W., Giri, D.D., Viale, A., Olshen, A.B., Gerald, W.L., and Massagué, J. (2005). Genes that mediate breast cancer metastasis to lung. *Nature* 436, 518–524.
- Naylor, T.L., Greshock, J., Wang, Y., Colligon, T., Yu, Q.C., Clemmer, V., Zaks, T.Z., and Weber, B.L. (2005). High resolution genomic analysis of sporadic breast cancer using array-based comparative genomic hybridization. *Breast Cancer Res.* 7, R1186–R1198.
- Park, H., Kim, Y., Lim, Y., Han, I., and Oh, E.S. (2002). Syndecan-2 mediates adhesion and proliferation of colon carcinoma cells. *J. Biol. Chem.* 277, 29730–29736.
- Pollack, J.R., Sorlie, T., Perou, C.M., Rees, C.A., Jeffrey, S.S., Lonning, P.E., Tibshirani, R., Botstein, D., Borresen-Dale, A.L., and Brown, P.O. (2002). Microarray analysis reveals a major direct role of DNA copy number alteration in the transcriptional program of human breast tumors. *Proc. Natl. Acad. Sci. USA* 99, 12963–12968.
- Ramaswamy, S., Ross, K.N., Lander, E.S., and Golub, T.R. (2003). A molecular signature of metastasis in primary solid tumors. *Nat. Genet.* 33, 49–54.
- Ried, T., Just, K.E., Holtgreve-Grez, H., du Manoir, S., Speicher, M.R., Schrock, E., Latham, C., Blegen, H., Zetterberg, A., Cremer, T., et al. (1995). Comparative genomic hybridization of formalin-fixed, paraffin-embedded breast tumors reveals different patterns of chromosomal gains and losses in fibroadenomas and diploid and aneuploid carcinomas. *Cancer Res.* 55, 5415–5423.
- Sreerama, L., and Sladek, N.E. (2001). Primary breast tumor levels of suspected molecular determinants of cellular sensitivity to cyclophosphamide, ifosfamide, and certain other anticancer agents as predictors of paired metastatic tumor levels of these determinants. Rational individualization of cancer chemotherapeutic regimens. *Cancer Chemother. Pharmacol.* 47, 255–262.
- Steeg, P.S. (2006). Tumor metastasis: mechanistic insights and clinical challenges. *Nat. Med.* 12, 895–904.
- Tanaka, S., Akaike, T., Fang, J., Beppu, T., Ogawa, M., Tamura, F., Miyamoto, Y., and Maeda, H. (2003). Antiapoptotic effect of haem oxygenase-1 induced by nitric oxide in experimental solid tumour. *Br. J. Cancer* 88, 902–909.
- van de Vijver, M.J., He, Y.D., van't Veer, L.J., Dai, H., Hart, A.A., Voskuil, D.W., Schreiber, G.J., Peterse, J.L., Roberts, C., Marton, M.J., et al. (2002). A gene-expression signature as a predictor of survival in breast cancer. *N. Engl. J. Med.* 347, 1999–2009.
- van't Veer, L.J., Dai, H., van de Vijver, M.J., He, Y.D., Hart, A.A., Mao, M., Peterse, H.L., van der Kooy, K., Marton, M.J., Witteveen, A.T., et al. (2002). Gene expression profiling predicts clinical outcome of breast cancer. *Nature* 415, 530–536.
- Wang, Y., Klijn, J.G., Zhang, Y., Sieuwerts, A.M., Look, M.P., Yang, F., Talantov, D., Timmermans, M., Meijer-van Gelder, M.E., Yu, J., et al. (2005). Gene-expression profiles to predict distant metastasis of lymph-node-negative primary breast cancer. *Lancet* 365, 671–679.
- Wei, Y., and Au, J.L.-S. (2005). Role of tumor microenvironment in mediating chemoresistance. In *Integration/Interaction of Oncologic Growth (Cancer Growth and Progression, Volume 15)*, G. Meadows, ed. (Boston: Kluwer Academic Publishers), pp. 285–321.
- Xu, L., Begum, S., Hearn, J.D., and Hynes, R.O. (2006). GPR56, an atypical G protein-coupled receptor, binds tissue transglutaminase, TG2, and inhibits melanoma tumor growth and metastasis. *Proc. Natl. Acad. Sci. USA* 103, 9023–9028.
- Yang, J., Mani, S.A., Donaher, J.L., Ramaswamy, S., Itzykson, R.A., Come, C., Savagner, P., Gitelman, I., Richardson, A., and Weinberg, R.A. (2004). Twist, a master regulator of morphogenesis, plays an essential role in tumor metastasis. *Cell* 117, 927–939.